J Cardiovasc Imaging. 2023 Apr;31(2):71-82
https://doi.org/10.4250/jcvi.2022.0080
pISSN 2586-7210·eISSN 2586-7296

Journal of Cardiovascular Imaging JCVI

Original Article

Dynamic Cardiac Magnetic Resonance Fingerprinting During Vasoactive Breathing Maneuvers: First Results

Luuk H.G.A. Hopman, Msc[1,2,*], Elizabeth Hillier, PhD[1,3,*], Yuchi Liu, PhD[4], Jesse Hamilton, PhD[4], Kady Fischer, PhD[5], Nicole Seiberlich, PhD[4,6], and Matthias G. Friedrich, MD, PhD[1,7]

[1]Research Institute of the McGill University Health Center, Montreal, QC, Canada
[2]Department of Cardiology, Amsterdam UMC, Amsterdam, The Netherlands
[3]Faculty of Medicine and Dentistry, University of Alberta, Edmonton, AB, Canada
[4]Department of Biomedical Engineering, Case Western Reserve University, Cleveland, OH, USA
[5]Department of Anaesthesiology and Pain Medicine, Bern University Hospital, Inselspital, University of Bern, Bern, Switzerland
[6]Department of Radiology, University Hospitals Cleveland Medical Center, Cleveland, OH, USA
[7]Departments of Cardiology and Diagnostic Radiology, McGill University Health Centre, Montreal, QC, Canada

Received: Jul 4, 2022
Revised: Aug 22, 2022
Accepted: Oct 10, 2022
Published online: Nov 10, 2022

Address for Correspondence:
Matthias G. Friedrich, MD, PhD
Departments of Cardiology and Diagnostic Radiology, McGill University Health Centre, 1001 Decarie Blvd., Montreal, QC H4A 3J1, Canada.
Email: mgwfriedrich@gmail.com

*Luuk H.G.A. Hopman and Elizabeth Hillier contributed equally to this manuscript.

ABSTRACT

BACKGROUND: Cardiac magnetic resonance fingerprinting (cMRF) enables simultaneous mapping of myocardial T1 and T2 with very short acquisition times. Breathing maneuvers have been utilized as a vasoactive stress test to dynamically characterize myocardial tissue *in vivo*. We tested the feasibility of sequential, rapid cMRF acquisitions during breathing maneuvers to quantify myocardial T1 and T2 changes.
METHODS: We measured T1 and T2 values using conventional T1 and T2-mapping techniques (modified look locker inversion [MOLLI] and T2-prepared balanced-steady state free precession), and a 15 heartbeat (15-hb) and rapid 5-hb cMRF sequence in a phantom and in 9 healthy volunteers. The $cMRF_{5\text{-}hb}$ sequence was also used to dynamically assess T1 and T2 changes over the course of a vasoactive combined breathing maneuver.
RESULTS: In healthy volunteers, the mean myocardial T1 of the different mapping methodologies were: MOLLI 1,224 ± 81 ms, $cMRF_{15\text{-}hb}$ 1,359 ± 97 ms, and $cMRF_{5\text{-}hb}$ 1,357 ± 76 ms. The mean myocardial T2 measured with the conventional mapping technique was 41.7 ± 6.7 ms, while for $cMRF_{15\text{-}hb}$ 29.6 ± 5.8 ms and $cMRF_{5\text{-}hb}$ 30.5 ± 5.8 ms. T2 was reduced with vasoconstriction (post-hyperventilation compared to a baseline resting state) (30.15 ± 1.53 ms vs. 27.99 ± 2.07 ms, p = 0.02), while T1 did not change with hyperventilation. During the vasodilatory breath-hold, no significant change of myocardial T1 and T2 was observed.
CONCLUSIONS: $cMRF_{5\text{-}hb}$ enables simultaneous mapping of myocardial T1 and T2, and may be used to track dynamic changes of myocardial T1 and T2 during vasoactive combined breathing maneuvers.

Keywords: Magnetic resonance imaging; Multiparametric magnetic resonance imaging; Myocardium; Breathing exercises

Journal of Cardiovascular Imaging JCVI

INTRODUCTION

Cardiovascular magnetic resonance (CMR) tissue characterization, specifically parametric mapping, has emerged as a method that can provide clinicians with a "virtual biopsy."[1] Fundamentally, CMR parametric mapping converts the intrinsic basic physical properties of myocardial tissue into magnetic relaxation times (T1 and T2), to provide quantitative pixelwise measurements (displayed as maps) of myocardial tissue. Conventional T1 and T2 mapping techniques are acquired independently as breath-hold sequences that take between 9 to 11 and 7 to 20 heartbeats for T1 and T2 mapping, respectively.[1]

Cardiac magnetic resonance fingerprinting (cMRF) is a novel acquisition technique that can simultaneously acquire T1 and T2 maps in a single acquisition.[2] cMRF uses varying acquisition parameters to impart a unique, complex pattern of signals ("fingerprint") to each type of tissue. After the data acquisition, a pattern recognition algorithm is used to search for matching patterns in a defined library. The best match indicates the tissue properties (and therefore the quantitative value) that should be assigned to each voxel, which are then converted into color coded T1 and T2 maps.[2] Additional iterations of cMRF have accelerated the acquisition to allow for the simultaneous acquisition of T1 and T2 maps in 15-hb.[3][4] The further reduction in acquisition time with a novel 5-hb cMRF acquisition represents the first opportunity for the assessment of both T1 and T2 mapping during a vasoactive stress CMR exam.

Previously, initial results from dynamic CMR stress T1 mapping had demonstrated an ability to differentiate between areas of ischemia and infarction from healthy or control myocardium in a patient population with suspected coronary artery disease (CAD),[5][6] and a blunted T1 stress response in patients with non-ischemic cardiomyopathy.[7] However, more recent findings suggest that performance of stress T1 mapping to differentiate between inducible ischemia and scar in a suspected CAD population is not reliable[6]; potentially in part due to methodologic or T1 mapping sequence differences.[8] Additionally, the use of adenosine as the vasoactive stress agent in dynamic mapping can have mild to severe side effects,[9] and these studies were performed with traditional CMR mapping techniques, limiting the acquisition to T1 only. While stress T1 mapping can detect changes in myocardial blood volume, stress T2 mapping is more sensitive to hemodynamic changes, including myocardial blood flow, oxygen consumption and venous blood oxygen levels.[10]

Respiratory challenges of inhaled gas mixtures, hyperventilation, or breath-holds, utilize the vasoactive properties of carbon dioxide and have demonstrated to be feasible and detectable vasoactive stimuli assessed using magnetic resonance imaging (MRI).[11][12] A combined breathing maneuver of one minute of paced hyperventilation, inducing vasoconstriction, followed by a maximal voluntary breath-hold, inducing vasodilation, has been shown to result in greater signal intensity changes than adenosine in healthy volunteers on MRI.[13] Recently, the combined breathing maneuver has been utilized as a vasoactive stimulus in the accurate detection of reduced oxygenation in affected myocardium in patients with both ischemic and non-ischemic cardiomyopathy states.[14-17]

We hypothesized that a combined breathing maneuver with a fast (5-hb) cMRF mapping acquisition could quantitatively assess dynamic changes in myocardial T1 and T2 in healthy participants, and thus potentially provide a needle-free alternative for CMR stress imaging.

METHODS

cMRF

Pulse sequence

The cMRF pulse sequence, as well as the dictionary generation and the pattern matching process, were used as previously described.[18] The cMRF sequence used for all phantom and *in vivo* experiments was based on a steady-state free-precession sequence (field of view 300 × 300 mm^2, matrix size 192 × 192, in-plane resolution 1.6 × 1.6 mm^2, slice thickness 8 mm). Data were acquired at end-diastole during breath-hold to reduce cardiac motion artefacts. At the beginning of every hb, a trigger delay is followed by a up to 255 ms acquisition window. During the scan, there is a constant repetition time (TR) of 5.1 ms and flip angles are varied between 4° and 25° to acquire the different signal evolutions and combinations of T1 and T2 values. An inversion pulse is applied every 5-hb with a constant inversion time of 21 ms, and T2 preparation pulses are played out in every third, fourth, and fifth hb of each 5-hb block with echo times of 30 ms, 50 ms, and 80 ms, respectively. A variable density spiral trajectory that rotates by the golden angle every TR was used to sample the k-space (R = 48).[19] The total number of highly undersampled maps acquired per scan was 750 for the cMRF$_{15\text{-hb}}$ sequence and 250 cMRF$_{5\text{-hb}}$ sequence.

Dictionary generation

For each voxel, the signal evolution over time was matched to a cMRF dictionary generated using a Bloch equation simulation with corrections for slice profile effects and imperfect preparation pulse (inversion and T2 preparation) efficiency.[20] In

https://doi.org/10.4250/jcvi.2022.0080

this dictionary, possible signal evolutions were linked to specific pairs of T1 and T2 values. A new dictionary covering the entire dynamic process was generated for each scan. To reconstruct dynamic maps during the breathing maneuver, a dictionary covering the entire dynamic process was generated with the simulated endpoint of the magnetization from the previous time frame as a starting point for the following time frame. Sixty seconds of dynamic cMRF raw data and the dictionary were divided into 5-hb segments and pattern-matching was then performed to generate the maps. All cMRF data were reconstructed using a low-rank method that constrains the cMRF signal time courses to a low-dimensional subspace calculated from the singular value decomposition of the dictionary.[21] The cMRF dictionaries were generated offline using MATLAB R2015a (MathWorks, Natick, MA, USA). After pattern matching, the combination of tissue properties that were used to generate the matching dictionary entry was assigned to that voxel. The tissue properties were then depicted as pixel-wise maps.

Study subjects and imaging protocol

MRI setup

All experiments were performed using a 3 Tesla clinical MRI system (Siemens MAGNETOM Skyra™; Siemens, Erlangen, Germany) using an 18-channel array coil.

International Society of Magnetic Resonance in Medicine/ National Institute of Standards and Technology (ISMRM/NIST) MRI system phantom

A validated MRI system phantom (ISMRM/NIST MRI system phantom; ISMRM/NIST, Gaithersburg, MD, USA) was used to compare the phantom-specific reference T1 and T2 values with cMRF-derived results. The phantom contained 14 vials with T1 values ranging from 90.9 ms to 2,480 ms and T2 values ranging from 5.6 ms to 581.3 ms.[22] An artificial heart rate was simulated at 60 beats per minute. The scans were performed with the $cMRF_{15\text{-}hb}$ sequence and the $cMRF_{5\text{-}hb}$ sequence.

The $cMRF_{5\text{-}hb}$ sequence was acquired in a dynamic fashion over 30 seconds, resulting in 6 consecutive sets of $cMRF_{5\text{-}hb}$ maps. Additionally, we simulated the heart rate change observed over a breath-hold in a healthy population, using a baseline value of 110 bpm and reducing it by 10 bpm every 5 seconds for the first 30 seconds and then keeping it at 60 bpm for the remaining 30 seconds. T1 and T2 maps were generated from both datasets and the values were compared to the gold standard NIST values using a linear regression test.

Healthy participants

Healthy participants were eligible to participate in the study if they did not meet the exclusion criteria, i.e., known cardiovascular disease, known respiratory disease, pregnancy or breastfeeding, or CMR contraindications (such as metal implants and claustrophobia). Nine healthy participants were enrolled between July 2018 and September 2018.

The CMR protocol included native T1 mapping, T2 mapping, and cMRF performed in a short axis orientation at a basal, mid-ventricular, and apical level. Dynamic cMRF during combined breathing maneuvers was performed in one short axis view at a mid-ventricular level. An 11-hb modified look locker inversion (MOLLI) sequence with a 5(3)3 acquisition scheme was used to generate standard T1 maps (acquisition window 281 ms, TE 1.12 ms, flip angle 35 deg, voxel size 1.5 × 1.5 × 6.0 mm, bandwidth 1,085 Hz/Px). A T2-prepared balanced steady state free precession (SSFP) sequence was used to generate T2 maps (acquisition window 207 ms, TE 1.32 ms, flip angle 12º, voxel size 1.9 × 1.9 × 6.0 mm, bandwidth 1,184 Hz/Px).

Following the conventional mapping and baseline cMRF (15-hb and 5-hb) data collection, dynamic cMRF maps were used to assess T1 and T2 value changes over time during the vasoactive breathing maneuver. Research participants performed a paced hyperventilation for 60 seconds at a rate of 30 breathing cycles per minute, followed by a voluntary long breath-hold of 60 seconds or more as previously described.[23] A metronome was used to ensure a reproducible breathing pattern during this period. The research team monitored adherence to the breathing maneuver through a camera in the scanner room. During the long breath-hold, a total of 60-hb of cMRF data were continuously acquired. The 60-hb cMRF data were split into twelve sets of 5-hb data to reconstruct a total of twelve T1 and T2 maps per participant (**Figure 1**). Each subject's cardiac rhythm was recorded from the external electrocardiogram (ECG) to generate the scan-specific cMRF dictionary.

Map analysis and blinding procedure

All resulting T1 and T2 maps were anonymized to the readers. T1 and T2 cMRF maps were calculated offline using MATLAB R2015a (MathWorks). After image reconstruction in MATLAB, DICOM files were created and the standard (MOLLI, T2 SSFP) and cMRF maps were analyzed using certified software (cvi[42]; Circle Cardiovascular Imaging, Inc., Calgary, Canada). Two experienced readers (LH and EH) manually drew region of interests over the entire myocardial wall to report global T1 and T2 values as well as segmental T1 and T2 values according to the American Heart Association 17 segment model. The mean and standard deviation (SD) in T1 and T2 values were calculated in these areas. One reader (EH) rated the image quality of each

Journal of Cardiovascular Imaging JCVI

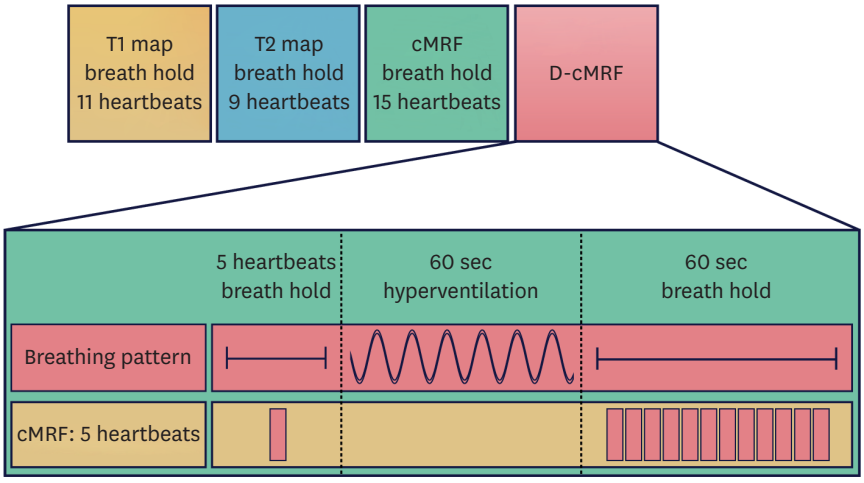

Figure 1. Magnetic resonance imaging protocol used to scan healthy volunteers.
cMRF: cardiac magnetic resonance fingerprinting, D-cMRF: dynamic cardiac magnetic resonance fingerprinting.

map out of 4 (1 = lowest, 4 = highest). As a result of import incompatibilities with multiple repeated images with the same Dicom tags, the dynamic cMRF maps were analysed in MATLAB by the same readers with the same methodology.

Statistical analysis

Results are presented as mean ± SD for normally distributed data and median including interquartile range for data that was not distributed normally. Normality of continuous data was assessed by the Shapiro-Wilks test and Q-Q plots. Pearson's correlation was used to quantify the association between continuous variables. Agreement between the phantom reference and cMRF values was assessed by intraclass correlation coefficients (ICCs) and by Bland-Altman analysis. ICCs for absolute agreement of single measurements were estimated using a 2-way mixed effect model. To test the influence of heart rate variance on measured $cMRF_{5\text{-}hb}$ T1 and T2 values, a linear regression test was performed on the log transformed data. Agreement between global and segmental T1 and T2 values derived from the $cMRF_{15\text{-}hb}$ and MOLLI, and the $cMRF_{15\text{-}hb}$ and T2-prepared balanced SSFP were evaluated by performing an independent samples t-test. Evaluation of pre-hyperventilation and post-hyperventilation cMRF maps was done using a paired t-test. Evaluation of overall image quality comparisons between the 15-hb cMRF, 5-hb cMRF, and MOLLI/T2-prepared balanced SSFP, and post-hyperventilation data were evaluated using a repeated measure analysis of variance test with Bonferroni post hoc testing. Data were considered significant if p-value < 0.05. Statistical analysis was performed using GraphPad™ Prism 7 (GraphPad Software Inc., La Jolla, CA, USA) and SPSS Statistics v26 (IBM Corporation, Armonk, NY, USA).

Ethics approval and consent to participate

Collection and management of data was approved by the local medical ethics committee (McGill University Health Centre Research Ethics Board, Quebec, Canada; Research Ethics Committee Reference Number 2020-6128). Informed consent was obtained from all individual participants included in the study.

RESULTS

Phantom imaging

The T1 and T2 values obtained with the $cMRF_{15\text{-}hb}$ and $cMRF_{5\text{-}hb}$ sequences showed a very strong agreement and linear correlation with the phantom T1 and T2 reference values (**Figure 2**) (ICC = 0.99 for $cMRF_{15\text{-}hb}$ T1, ICC = 0.99 for $cMRF_{5\text{-}hb}$ T1, ICC = 0.98 for $cMRF_{15\text{-}hb}$ T2, and ICC = 0.97 for $cMRF_{5\text{-}hb}$ T2).

For the $cMRF_{5\text{-}hb}$ sequence over 30-hb, in the range of human myocardial T1 and T2 (700 ms < T1 < 1,500 ms, 25 ms < T2 < 80 ms), the ICC was 0.99 for T1 and 0.98 for T2 (**Supplementary Figure 1**). The coefficient of variation, defined as the ratio of the SD to the mean, for each T1 and T2 value is displayed in **Supplementary Table 1**.

In the dynamic cMRF scan with a simulated decrease in the heart rate, the observed values in the physiological range of T1 and T2 varied slightly (**Supplementary Figure 2**). The difference between the phantom's reference values and the measured T1 ($p = 0.05$) and T2 ($p = 0.64$) values could not be explained by heart rate variance.

https://doi.org/10.4250/jcvi.2022.0080

Journal of Cardiovascular Imaging JCVI

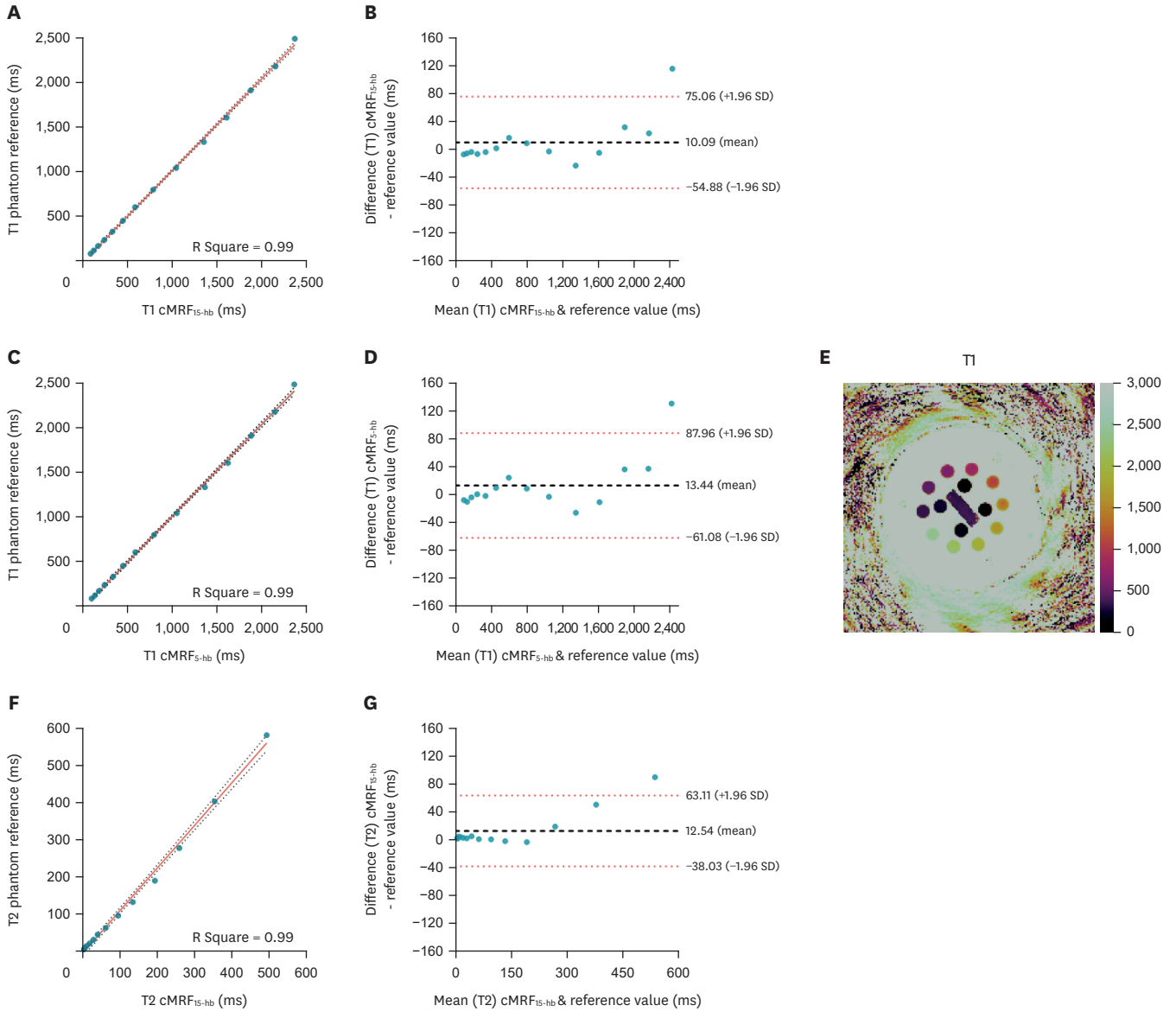

Figure 2. Phantom results. (A) Results of the $cMRF_{15\text{-}hb}$ sequence compared to the phantom T1 reference values. (B) Bland-Altman plot to describe agreement between the $cMRF_{15\text{-}hb}$ T1 values and the phantom T1 reference values. The solid black line indicated the mean bias and the dashed red lines indicate the limits of agreement. (C) Results of the $cMRF_{5\text{-}hb}$ sequence compared to the phantom T1 reference values. (D) Bland-Altman plot to describe agreement between the $cMRF_{5\text{-}hb}$ T1 values and the phantom T1 reference values. The solid black line indicated the mean bias and the dashed red lines indicate the limits of agreement. (E) T1 map of the phantom acquired with the $cMRF_{15\text{-}hb}$ sequence. (F) Results of the $cMRF_{15\text{-}hb}$ sequence compared to the phantom T2 reference values. (G) Bland-Altman plot to describe agreement between the $cMRF_{15\text{-}hb}$ T2 values and the phantom T2 reference values. The solid black line indicated the mean bias and the dashed red lines indicate the limits of agreement. (H) Results of the $cMRF_{5\text{-}hb}$ sequence compared to the phantom T2 reference values. (I) Bland-Altman plot to describe agreement between the $cMRF_{5\text{-}hb}$ T2 values and the phantom T2 reference values. The solid black line indicated the mean bias and the dashed red lines indicate the limits of agreement. (J) T2 map of the phantom acquired with the $cMRF_{15\text{-}hb}$ sequence.
cMRF: cardiac magnetic resonance fingerprinting, hb: heartbeat.

(continued to the next page)

Human volunteer imaging

All 9 volunteers successfully completed the conventional, 15-hb and 5-hb cMRF maps, and 8 healthy volunteers completed the dynamic cMRF with vasoactive breathing maneuvers. In one healthy volunteer, dynamic cMRF could not be performed because of ECG trigger problems. In 2 male healthy volunteers, a non-adiabatic T2 preparation was used instead of an adiabatic preparation to stay within specific absorption rate limits. All maps were analysed except for a total of 3 slices (2 apical slices and 1 basal slice) of the conventional mapping images and 4 slices (1 basal slice, 1 mid slice, and 2 apical slices) of the cMRF maps, due to poor image quality (i.e., artefacts). Overall

https://doi.org/10.4250/jcvi.2022.0080

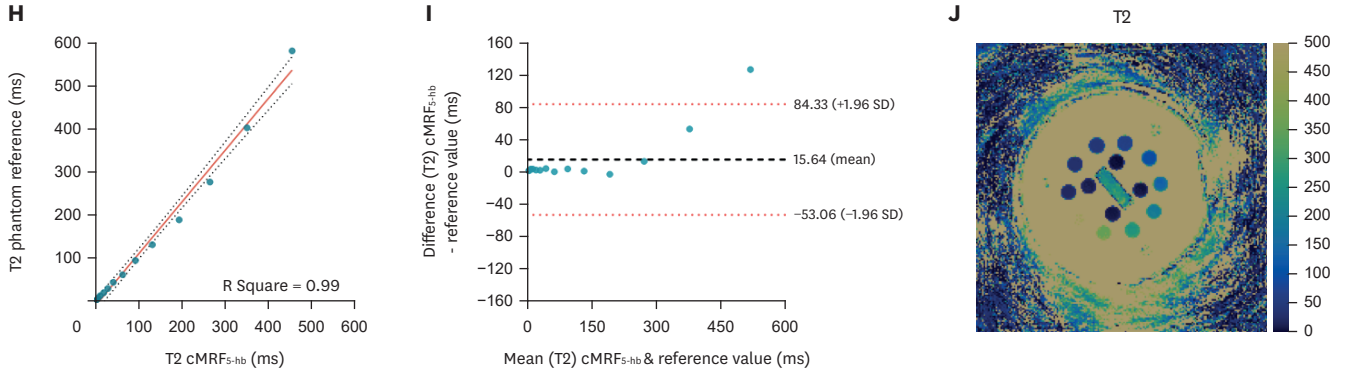

Figure 2. (Continued) Phantom results. (A) Results of the $cMRF_{15\text{-}hb}$ sequence compared to the phantom T1 reference values. (B) Bland-Altman plot to describe agreement between the $cMRF_{15\text{-}hb}$ T1 values and the phantom T1 reference values. The solid black line indicated the mean bias and the dashed red lines indicate the limits of agreement. (C) Results of the $cMRF_{5\text{-}hb}$ sequence compared to the phantom T1 reference values. (D) Bland-Altman plot to describe agreement between the $cMRF_{5\text{-}hb}$ T1 values and the phantom T1 reference values. The solid black line indicated the mean bias and the dashed red lines indicate the limits of agreement. (E) T1 map of the phantom acquired with the $cMRF_{15\text{-}hb}$ sequence. (F) Results of the $cMRF_{15\text{-}hb}$ sequence compared to the phantom T2 reference values. (G) Bland-Altman plot to describe agreement between the $cMRF_{15\text{-}hb}$ T2 values and the phantom T2 reference values. The solid black line indicated the mean bias and the dashed red lines indicate the limits of agreement. (H) Results of the $cMRF_{5\text{-}hb}$ sequence compared to the phantom T2 reference values. (I) Bland-Altman plot to describe agreement between the $cMRF_{5\text{-}hb}$ T2 values and the phantom T2 reference values. The solid black line indicated the mean bias and the dashed red lines indicate the limits of agreement. (J) T2 map of the phantom acquired with the $cMRF_{15\text{-}hb}$ sequence.
cMRF: cardiac magnetic resonance fingerprinting, hb: heartbeat.

image quality was rated higher for the 15-hb cMRF maps when compared to standard mapping sequences for both T1 (cMRF: 2.89 ± 0.7; MOLLI: 2.56 ± 0.6, p = 0.03) and T2 (cMRF: 2.81 ± 0.9; T2-prepared balanced SSFP: 2.44 ± 0.8, p = 0.03). There was no significant difference in overall image quality between the 15-hb and 5-hb cMRF maps, or between the 5-hb cMRF maps and the MOLLI or T2-prepared balanced SSFP sequence, p > 0.05.

Baseline characteristics of the healthy volunteers are displayed in **Table 1**. Approximately half of our population was female, and the mean age was 38 ± 13 years. **Figure 3** displays representative T1 and T2 maps from one volunteer acquired with conventional mapping techniques, the 15-hb, and the 5-hb cMRF sequences.

Table 2 and **Figure 4** show the T1 and T2 values of the different acquisition techniques. There was no difference in mean myocardial T1 or T2 values between the $cMRF_{15\text{-}hb}$ sequence and the $cMRF_{5\text{-}hb}$ sequence (T1: p = 0.92; T2: p = 0.34). The global myocardial T1 values obtained with the 15-hb (1,359 ± 97 ms, p < 0.01) and 5-hb (1,357 ± 76 ms, p < 0.01) cMRF sequence were higher than the global T1 measured with MOLLI (1,224 ± 81 ms). The global T2 values obtained with the 15-hb (29.6 ± 5.8 ms, p < 0.01) and 5-hb (30.5 ± 5.8 ms, p < 0.01) cMRF sequence were lower than the global T2 measured with the standard T2-prepared balanced SSFP sequence (41.7 ± 6.7 ms).

Table 1. Characteristics of the healthy volunteers

Characteristics	Healthy volunteers (n = 9)
Age (years)	38 ± 13
Male (%)	4/9 (44%)
Weight (kg)	69.4 ± 15.2
Height (m)	1.72 ± 0.11
BMI (kg/m^2)	23.4 ± 4.5

All values are mean ± standard deviation for continuous variables and number (%) for categorical variables.
BMI: body mass index calculated by dividing weight by height^2.

Dynamic MRF

Eight healthy volunteers had images acquired throughout, and successfully completed, the vasoactive breathing maneuver. The subjects did not report any adverse effects during or after the breathing maneuvers.

T1 values did not differ between baseline $cMRF_{5\text{-}hb}$ (1,352.21 ± 32.28 ms) and post-hyperventilation $cMRF_{5\text{-}hb}$ (1,360 ± 45.52 ms, p = 0.49) maps. T2 values were significantly lower post-hyperventilation compared to the baseline, resting state measurement (27.99 ± 2.07 ms vs. 30.15 ± 1.53 ms, p = 0.02) (**Figure 5**). No significant effect in myocardial T1 and T2 values (Wilks' Lambda for T1 = 0.65, for T2 = 0.53) was observed during the post-hyperventilation breath hold (**Supplementary Figure 3**). However, myocardial T2 increased 12.8% (27.99 ± 2.07 ms at baseline to 31.57 ± 2.75 ms at 60 seconds into the breath-hold) over the breath-hold (**Figure 5B**).

DISCUSSION

In this proof-of-concept study, we have shown that a fast $cMRF_{5\text{-}hb}$ sequence allows for rapid yet accurate mapping of myocardial T1 and T2, when compared to a longer $cMRF_{15\text{-}hb}$ acquisition. We have also shown that stress cMRF mapping, mapping

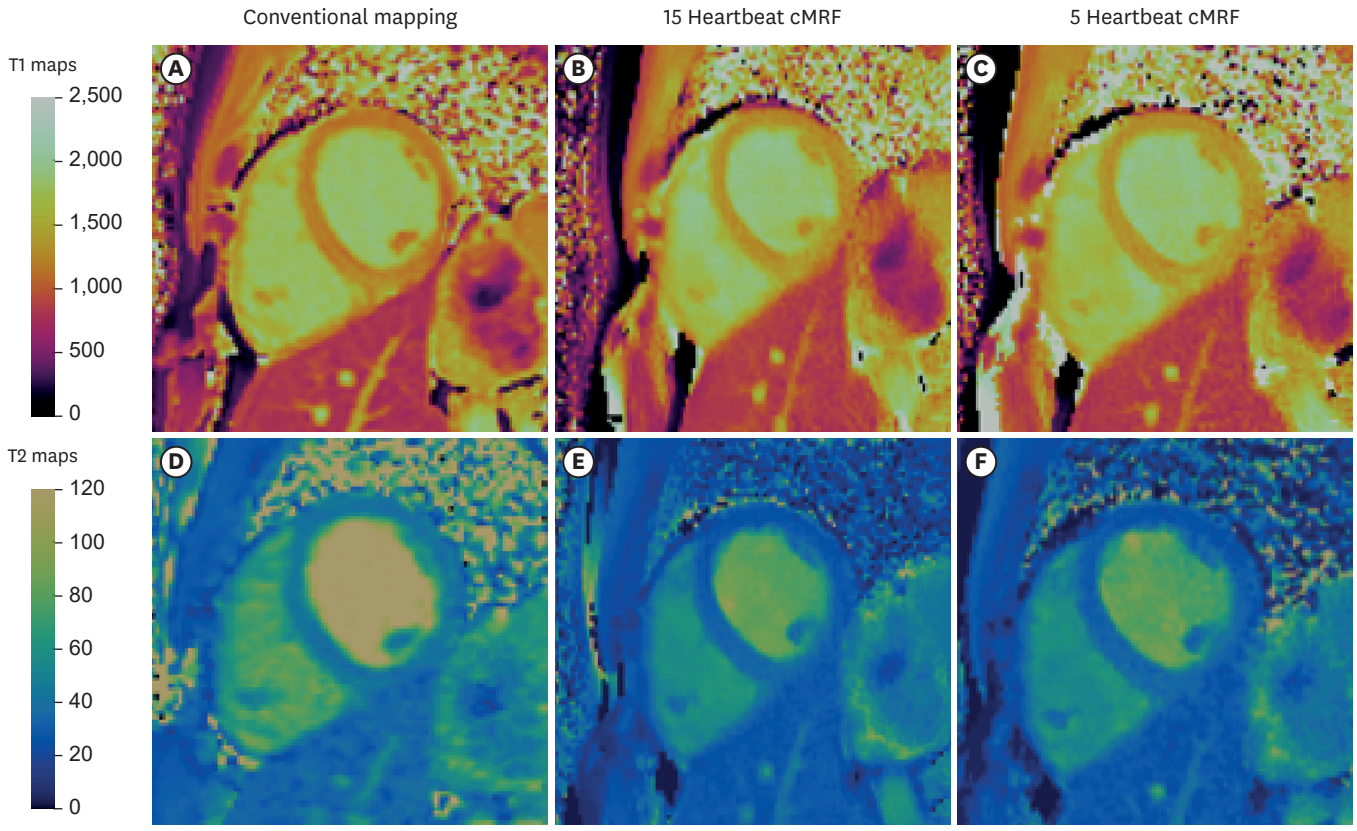

Figure 3. Comparison of T1 and T2 maps in a healthy volunteer. The maps represent results acquired using conventional techniques: (A) T1: MOLLI, (D) T2: T2 prepared balanced SSFP sequence; and cMRF maps acquired using the 15-hb protocol (B, E), and the 5-hb protocol (C, F).
cMRF: cardiac magnetic resonance fingerprinting, hb: heartbeat, MOLLI: modified look locker inversion, SSFP: steady state free precession.

Table 2. Mean T1 and T2 values measured with conventional mapping techniques and cMRF

Characteristics	MOLLI (ms)*	T2-prepared balanced SSFP (ms)*	$cMRF_{15\text{-}hb}$ (ms)*	$cMRF_{5\text{-}hb}$ (ms)	p-value between $cMRF_{15\text{-}hb}$ and $cMRF_{5\text{-}hb}$
Mean T1 value global	1,224 ± 81		1,359 ± 97	-	
Mean T1 value basal segments	1,220 ± 82		1,361 ± 97	-	
Mean T1 value mid segments	1,220 ± 84		1,353 ± 94	1,357 ± 76	0.90
Mean T1 value apical segments	1,231 ± 7		1,355 ± 102	-	
Mean T2 value global		41.7 ± 6.7	29.6 ± 5.8	-	
Mean T2 value basal segments		41.7 ± 6.6	29.7 ± 5.6	-	
Mean T2 value mid segments		41.6 ± 6.3	29.7 ± 5.6	30.5 ± 5.8	0.54
Mean T2 value apical segments		41.2 ± 5.8	29.4 ± 6.3	-	

All values are mean ± standard deviation for continuous variables and number (%) for categorical variables.
cMRF: cardiac magnetic resonance fingerprinting, hb: heartbeat, MOLLI: modified look locker inversion, SSFP: steady state free precession.
*The p-values between conventional mapping techniques and cMRF were all < 0.001.

in combination with a vasoactive breathing maneuver, can dynamically assess and quantify an inducible coronary vascular response to stress in a healthy population.

Both the $cMRF_{15\text{-}hb}$ and $cMRF_{5\text{-}hb}$ sequence showed excellent correlation with the reference values for T1 and T2. In addition, using the $cMRF_{5\text{-}hb}$ in a consecutive manner gave consistent results over time. No relationship between heart rate variation and measured T1 and T2 values in the dynamic cMRF acquisition was observed when an artificially decreasing heart rate, mimicking the heart rate decrease in healthy humans during the breathing maneuver, was used.

In healthy volunteers, no difference in myocardial T1 and T2 values was observed between the regular and rapid cMRF sequence. Mean T1 relaxation times measured with cMRF were significantly higher than the results obtained by MOLLI T1. This is consistent with previous results which have described that the T1 underestimation by MOLLI when compared to both cMRF and saturation recovery single-shot acquisition, may result from

https://doi.org/10.4250/jcvi.2022.0080

Journal of Cardiovascular Imaging JCVI

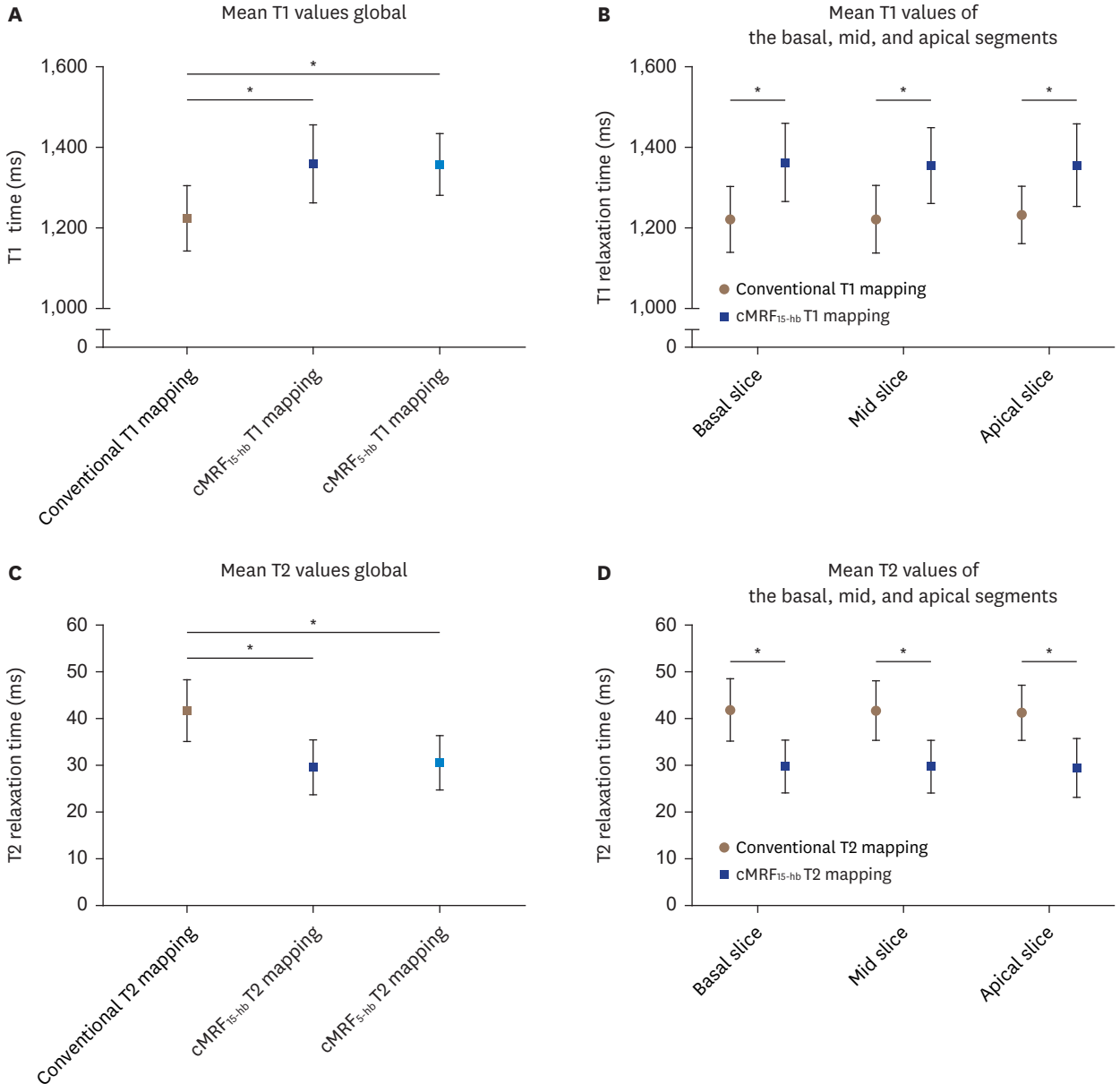

Figure 4. Comparison of T1 and T2 values between conventional mapping techniques and cMRF. Quantitative comparison of T1 between MOLLI cMRF$_{15\text{-hb}}$ and cMRF$_{5\text{-hb}}$ (A, B), and of T2 between cMRF$_{15\text{-hb}}$ and cMRF$_{5\text{-hb}}$ and a T2 prepared balanced SSFP sequence (C, D).
cMRF: cardiac magnetic resonance fingerprinting, hb: heartbeat, MOLLI: modified look locker inversion, SSFP: steady state free precession.
*$p < 0.01$.

magnetization transfer, the imperfect T2-dependent inversion efficiency, heart rate, and off resonance sensitivity of MOLLI.[20] The myocardial T2 values as derived from cMRF maps were lower than the values from T2-prepared balanced SSFP maps in our study. This finding is also consistent with previous results and likely due to intravoxel dephasing, magnetization transfer, and motion sensitivity along the slice direction of the T2-prepared balanced SSFP sequence.[24]

We have shown that a combined breathing maneuver of hyperventilation (inducing vasoconstriction) followed by a period of voluntary apnea (inducing vasodilation) induces a coronary vascular response measurable by dynamic cMRF T1 and T2 mapping. From a physiologic perspective, the positive relationship between T2 signal and myocardial water content has been previously described; where increased myocardial edema results in an increase in T2 signal and vice versa.

https://doi.org/10.4250/jcvi.2022.0080

Journal of Cardiovascular Imaging JCVI

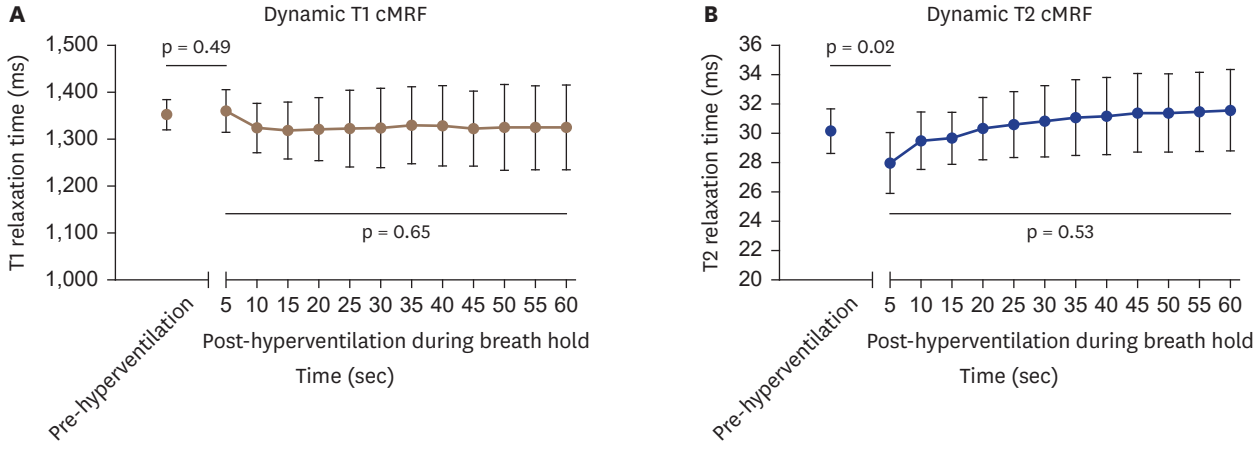

Figure 5. Dynamic cMRF in healthy volunteers during breathing manoeuvre. Myocardial relaxation times T1 (A) and T2 (B) pre-hyperventilation and during a post-hyperventilation breath-hold as measured by dynamic cMRF mapping.
cMRF: cardiac magnetic resonance fingerprinting.

Therefore, with hyperventilation induced vasoconstriction there is a resultant relative reduction in myocardial blood flow. This reduction in myocardial blood flow is then reversed during breath-hold induced vasodilatation resulting in a relative increase in myocardial blood flow.

Myocardial T2 values, which are significantly affected by myocardial blood flow, were reduced after a period of hyperventilation and increased back to baseline over the period a breath hold.[25] This reduction of T2 after a period of hyperventilation induced vasoconstriction is consistent with previous findings demonstrating that vasoconstriction induced by hyperventilation, reflects a reduction of myocardial blood flow, and therefore reduction in T2 signal intensity.[13]

While statistically not significant, an increase in T2 during a breath hold was observed when hb-to-hb quantitative T2 maps were acquired in healthy volunteers. During the long breath-hold, inducing vasodilation, an influx of blood with a high native T2 value resulted in a higher overall myocardial T2 value when compared to rest. This observation is concordant with previously published results by van den Boomen et al.[26]

The results of our study illicit further discussion around the impact of myocardial blood flow on both T1 and T2 values. As both T1 and T2 values are impacted by myocardial blood flow, the significant reduction in cMRF derived T2 and no significant change in cMRF derived T1 after hyperventilation may be unexpected. However, this is in line with previous results and discussion around the lower sensitivity of stress T1 mapping to hemodynamic changes when compared to T2.[10] Initial results demonstrated a significant potential for the dynamic assessment of myocardial perfusion by stress T1 mapping.[27] However, conflicting results and potential T1 mapping sequence differences have shown that stress T1 mapping may provide a better assessment of myocardial blood volume instead of dynamic myocardial blood flow,[5][6] and that stress T2 mapping is more sensitive to changes in myocardial blood flow.[10]

Data obtained in this study demonstrated that both the 15-hb and the 5-hb cMRF sequences provide both T1 and T2 myocardial relaxation time maps in a much shorter scan time than conventional mapping. Additionally, dynamic T2 cMRF stress mapping with vasoactive breathing maneuvers may offer an alternative to first pass perfusion imaging that does not require contrast or pharmaceutical stress agents, which may further reduce scan times. Future studies looking at patients with reduced kidney function, or those with prior severe reactions to pharmaceutical stress agents may serve to further highlight the widespread utility and reduction in overall scan time of this methodology when compared to conventional mapping and CMR perfusion imaging. Furthermore, the needle-free dynamic CMR stress test methodology used in this study utilizing a vasoactive breathing maneuver and a novel, 5-hb cMRF sequence should be tested for its clinical utility in the assessment of coronary vascular function.

A small number of volunteers participated in this study which limits the robustness of the study data. Moreover, we did not perform repeated scanning of the phantom and healthy volunteers which limits assessment of reproducibility of this novel imaging technique. Secondly, it has previously been suggested that the single model fit effect of the MOLLI 5(3)3 sequence has made this technique sensitive to changes in

https://doi.org/10.4250/jcvi.2022.0080

heart rate.[28] The role of heart rate variations on the effects of cMRF T1 and T2 values over a period of stress-inducing breathing maneuvers cannot be fully ruled out in the current study. However, cMRF has previously shown to have a high degree of independence from heart rate as the acquisition inherently incorporates heart rate timing of each heart beat into the data dictionary generation.[23] Thirdly, the studied cMRF technique does not include T2* mapping, which may be added in the future to achieve a higher sensitivity to track myocardial oxygenation changes. Additionally, the higher T1 and lower T2 values acquired from cMRF compared with the standard mapping techniques may represent an obstacle for widespread implementation or use. However, currently normal values for each site and individual scanner must be obtained for standard mapping techniques. Comparatively, the control of confounders present in the post-processing and reconstruction of cMRF may allow for site and vendor agnostic T1 and T2 values in the future, ultimately decreasing the obstacles currently faced for current parametric mapping implementation.[20] Finally, the cMRF data reconstruction is performed offline, making it not possible to assess the image quality of maps immediately at the MRI workstation. While image quality was not a problem in our study, ongoing developments may allow for a near real-time display of maps using neural network dictionary generation.[29][30] Future studies incorporating more healthy subjects and a patient population are warranted to validate the presented data and further elucidate the potential clinical implications and uses of needle-free, stress T1 and T2 mapping.

In conclusion, cardiac MR Fingerprinting using a fast, 5-hb cMRF sequence enables a rapid and accurate quantification of myocardial T1 and T2. Furthermore, our study showed its utility for dynamic monitoring of T1 and T2 during dynamic maneuvers such as changes of myocardial T2 during a post-hyperventilation breath-hold.

SUPPLEMENTARY MATERIALS

Supplementary Table 1

Dynamic T1 and T2 $cMRF_{5\text{-}hb}$ phantom values over 30 hbs (physiological range of T1 and T2)

Click here to view

Supplementary Figure 1

Dynamic cMRF in a phantom. (A) The precision of dynamic cMRF over 6 consecutive measurements displaying T1 values. (B) The precision of dynamic cMRF over 6 consecutive measurements displaying T2 values. Each measurement lasted 5 seconds at an artificially simulated heart rate at 60 beats per minute.

Click here to view

Supplementary Figure 2

Dynamic cMRF in a phantom during a decreasing heart rate (physiological range of T1 and T2). (A) T1 values measured during a decreasing heart rate. (B) T2 values measured during a decreasing heart rate. For the decreasing heart rate, a stepwise decrease of 110, 100, 90, 80, 70, 60 beats per minute every up to 5 seconds for the first 30 seconds, and 60 beats per minute for the remaining 30 seconds was used. The T1 and T2 reference values for each vial are displayed at the right side of graphs.

Click here to view

Supplementary Figure 3

Dynamic cMRF on an individual level. Myocardial relaxation times T1 (A) and T2 (B) during a post-hyperventilation breath-hold as measured by dynamic cMRF mapping for all eight healthy volunteers. A trend towards a decrease in T1 values is seen during breath hold. Healthy volunteer 7 demonstrates a remarkable, and possibly incorrectly measured, evolution of myocardial T1 values over time. A trend towards an increase in T2 values is seen during the breath hold.

Click here to view

ORCID iDs

Luuk H.G.A. Hopman
https://orcid.org/0000-0002-3896-9920
Elizabeth Hillier
https://orcid.org/0000-0003-2837-4680
Yuchi Liu
https://orcid.org/0000-0003-3533-1697
Jesse Hamilton
https://orcid.org/0000-0002-4463-481X
Kady Fischer
https://orcid.org/0000-0002-7765-4550
Nicole Seiberlich
https://orcid.org/0000-0002-8356-5407
Matthias G. Friedrich
https://orcid.org/0000-0003-1204-5647

Funding

This Fingerprinting study has been initiated by Matthias Friedrich with financial support from the McGill University Health Centre Foundation through the Courtois CMR Research Program.

Conflict of Interest

Matthias G. Friedrich is listed as a holder of United States Patent No. 14/419,877: Inducing and measuring myocardial oxygenation changes as a marker for heart

disease; United States Patent No. 15/483,712: Measuring oxygenation changes in tissue as a marker for vascular function; United States Patent No. 10,653,394: Measuring oxygenation changes in tissue as a marker for vascular function - continuation; and Canadian Patent CA2020/051776: Method and apparatus for determining biomarkers of vascular function utilizing bold CMR images.

Elizabeth Hillier is listed as a holder of International Patent CA2020/051776: Method and apparatus for determining biomarkers of vascular function utilizing bold CMR images.

Nicole Seiberlich receives research support from Siemens Healthineers. Siemens also licenses the MR Fingerprinting IP.

The funding sources were not involved in the study design; collection, analysis and interpretation of data; in the writing of the report; and in the decision to submit the article for publication.

All other authors declare that they have no competing interests.

Author Contributions

Conceptualization: Hopman LHGA, Hillier E, Fischer K, Seiberlich N, Friedrich MG; Data curation: Hopman LHGA, Hillier E; Formal analysis: Hopman LHGA, Hillier E, Liu Y; Investigation: Hopman LHGA, Hillier E; Methodology: Hopman LHGA, Hillier E, Fischer K; Resources: Liu Y, Hamilton J; Software: Liu Y, Hamilton J; Supervision: Hillier E, Liu Y, Fischer K, Seiberlich N, Friedrich MG; Validation: Liu Y; Writing - original draft: Hopman LHGA, Hillier E; Writing - review & editing: Liu Y, Hamilton J, Fischer K, Seiberlich N, Friedrich MG.

REFERENCES

1. Messroghli DR, Moon JC, Ferreira VM, et al. Clinical recommendations for cardiovascular magnetic resonance mapping of T1, T2, T2* and extracellular volume: a consensus statement by the Society for Cardiovascular Magnetic Resonance (SCMR) endorsed by the European Association for Cardiovascular Imaging (EACVI). *J Cardiovasc Magn Reson* 2017;19:75.
PUBMED | CROSSREF
2. Ma D, Gulani V, Seiberlich N, et al. Magnetic resonance fingerprinting. *Nature* 2013;495:187-92.
PUBMED | CROSSREF
3. Cruz G, Jaubert O, Botnar RM, Prieto C. Cardiac magnetic resonance fingerprinting: technical developments and initial clinical validation. *Curr Cardiol Rep* 2019;21:91.
PUBMED | CROSSREF
4. Liu Y, Hamilton J, Rajagopalan S, Seiberlich N. Cardiac magnetic resonance fingerprinting: technical overview and initial results. *JACC Cardiovasc Imaging* 2018;11:1837-53.
PUBMED | CROSSREF
5. Yimcharoen S, Zhang S, Kaolawanich Y, Tanapibunpon P, Krittayaphong R. Clinical assessment of adenosine stress and rest cardiac magnetic resonance T1 mapping for detecting ischemic and infarcted myocardium. *Sci Rep* 2020;10:14727.
PUBMED | CROSSREF
6. Bohnen S, Prüßner L, Vettorazzi E, et al. Stress T1-mapping cardiovascular magnetic resonance imaging and inducible myocardial ischemia. *Clin Res Cardiol* 2019;108:909-20.
PUBMED | CROSSREF
7. Cavallo AU, Liu Y, Patterson A, et al. CMR fingerprinting for myocardial T1, T2, and ECV quantification in patients with nonischemic cardiomyopathy. *JACC Cardiovasc Imaging* 2019;12:1584-5.
PUBMED | CROSSREF
8. Burrage MK, Shanmuganathan M, Zhang Q, et al. Cardiac stress T1-mapping response and extracellular volume stability of MOLLI-based T1-mapping methods. *Sci Rep* 2021;11:13568.
PUBMED | CROSSREF
9. Thomas DM, Minor MR, Aden JK, Lisanti CJ, Steel KE. Effects of adenosine and regadenoson on hemodynamics measured using cardiovascular magnetic resonance imaging. *J Cardiovasc Magn Reson* 2017;19:96.
PUBMED | CROSSREF
10. Weyers JJ, Ramanan V, Javed A, et al. Myocardial blood flow is the dominant factor influencing cardiac magnetic resonance adenosine stress T2. *NMR Biomed* 2022;35:e4643.
PUBMED | CROSSREF
11. Yang HJ, Yumul R, Tang R, et al. Assessment of myocardial reactivity to controlled hypercapnia with free-breathing T2-prepared cardiac blood oxygen level-dependent MR imaging. *Radiology* 2014;272:397-406.
PUBMED | CROSSREF
12. Kassner A, Winter JD, Poublanc J, Mikulis DJ, Crawley AP. Blood-oxygen level dependent MRI measures of cerebrovascular reactivity using a controlled respiratory challenge: reproducibility and gender differences. *J Magn Reson Imaging* 2010;31:298-304.
PUBMED | CROSSREF
13. Fischer K, Guensch DP, Friedrich MG. Response of myocardial oxygenation to breathing manoeuvres and adenosine infusion. *Eur Heart J Cardiovasc Imaging* 2015;16:395-401.
PUBMED | CROSSREF
14. Hillier E, Friedrich MG. The potential of oxygenation-sensitive CMR in heart failure. *Curr Heart Fail Rep* 2021;18:304-14.
PUBMED | CROSSREF
15. Ochs MM, Kajzar I, Salatzki J, et al. Hyperventilation/breath-hold maneuver to detect myocardial ischemia by strain-encoded CMR: diagnostic accuracy of a needle-free stress protocol. *JACC Cardiovasc Imaging* 2021;14:1932-44.
PUBMED | CROSSREF
16. Fischer K, Guensch DP, Jung B, et al. Insights into myocardial oxygenation and cardiovascular magnetic resonance tissue biomarkers in heart failure with preserved ejection fraction. *Circ Heart Fail* 2022;15:e008903.
PUBMED | CROSSREF
17. Spicher B, Fischer K, Zimmerli ZA, et al. Combined analysis of myocardial deformation and oxygenation detects inducible ischemia unmasked by breathing maneuvers in chronic coronary syndrome. *Front Cardiovasc Med* 2022;9:800720.
PUBMED | CROSSREF
18. Hamilton JI, Jiang Y, Chen Y, et al. MR fingerprinting for rapid quantification of myocardial T_1, T_2, and proton spin density. *Magn Reson Med* 2017;77:1446-58.
PUBMED | CROSSREF
19. Winkelmann S, Schaeffter T, Koehler T, Eggers H, Doessel O. An optimal radial profile order based on the Golden Ratio for time-resolved MRI. *IEEE Trans Med Imaging* 2007;26:68-76.
PUBMED | CROSSREF
20. Hamilton JI, Jiang Y, Ma D, et al. Investigating and reducing the effects of confounding factors for robust T_1 and T_2 mapping with cardiac MR fingerprinting. *Magn Reson Imaging* 2018;53:40-51.
PUBMED | CROSSREF
21. Hamilton JI, Jiang Y, Ma D, et al. Simultaneous multislice cardiac magnetic resonance fingerprinting using low rank reconstruction. *NMR Biomed* 2019;32:e4041.
PUBMED | CROSSREF

22. Jiang Y, Ma D, Keenan KE, Stupic KF, Gulani V, Griswold M. Repeatability of magnetic resonance fingerprinting T_1 and T_2 estimates assessed using the ISMRM/NIST MRI system phantom. *Magn Reson Med* 2017;78:1452-7.
PUBMED | CROSSREF

23. Hillier E, Covone J, Friedrich MG. Oxygenation-sensitive cardiac MRI with vasoactive breathing maneuvers for the non-invasive assessment of coronary microvascular dysfunction. *J Vis Exp* 2022;e64149.
PUBMED | CROSSREF

24. Hamilton JI, Pahwa S, Adedigba J, et al. Simultaneous mapping of T_1 and T_2 using cardiac magnetic resonance fingerprinting in a cohort of healthy subjects at 1.5T. *J Magn Reson Imaging* 2020;52:1044-52.
PUBMED | CROSSREF

25. Eitel I, Friedrich MG. T2-weighted cardiovascular magnetic resonance in acute cardiac disease. *J Cardiovasc Magn Reson* 2011;13:13.
PUBMED | CROSSREF

26. van den Boomen M, Manhard MK, Snel GJ, et al. Blood oxygen level-dependent MRI of the myocardium with multiecho gradient-echo spin-echo imaging. *Radiology* 2020;294:538-45.
PUBMED | CROSSREF

27. Liu A, Wijesurendra RS, Francis JM, et al. Adenosine stress and rest T1 mapping can differentiate between ischemic, infarcted, remote, and normal myocardium without the need for gadolinium contrast agents. *JACC Cardiovasc Imaging* 2016;9:27-36.
PUBMED | CROSSREF

28. Piechnik SK, Neubauer S, Ferreira VM. State-of-the-art review: stress T1 mapping-technical considerations, pitfalls and emerging clinical applications. *MAGMA* 2018;31:131-41.
PUBMED | CROSSREF

29. Hamilton JI, Seiberlich N. Machine learning for rapid magnetic resonance fingerprinting tissue property quantification. *Proc IEEE Inst Electr Electron Eng* 2020;108:69-85.
PUBMED | CROSSREF

30. Hamilton JI. A self-supervised deep learning reconstruction for shortening the breathhold and acquisition window in cardiac magnetic resonance fingerprinting. *Front Cardiovasc Med* 2022;9:928546.
PUBMED | CROSSREF